Nonclassical emission from single colloidal nanocrystals in a microcavity: a route towards room temperature single photon sources

2009 New J. Phys. 11 033025

(http://iopscience.iop.org/1367-2630/11/3/033025)

New Journal of Physics
The open-access journal for physics

Nonclassical emission from single colloidal nanocrystals in a microcavity: a route towards room temperature single photon sources

Antonio Qualtieri[1,4], Giovanni Morello[1], Piernicola Spinicelli[2], Maria T Todaro[1], Tiziana Stomeo[1], Luigi Martiradonna[1], Milena De Giorgi[1], Xavier Quélin[3], Stéphanie Buil[3], Alberto Bramati[2], Jean P Hermier[2,3], Roberto Cingolani[1] and Massimo De Vittorio[1]

[1] National Nanotechnology Laboratory (NNL) of CNR-INFM, Distretto Tecnologico ISUFI, Università del Salento, via per Arnesano, 73100 Lecce, Italy
[2] Laboratoire Kastler Brossel—Université Paris 6, Ecole Normale Supérieure et CNRS, UPMC case 74, 4 Place Jussieu, 75252 Paris Cedex 05, France
[3] Groupe d'étude de la Matière Condensée, CNRS UMR8635, Université de Versailles Saint Quentin, 45 avenue des Etats-Unis, 78035 Versailles Cedex, France
E-mail: antonio.qualtieri@unile.it

New Journal of Physics **11** (2009) 033025 (9pp)
Received 4 December 2008
Published 20 March 2009
Online at http://www.njp.org/
doi:10.1088/1367-2630/11/3/033025

Abstract. Secure quantum communication systems (QCS) based on the transmission of crucial information through single photons are among the most appealing frontiers for telecommunications, though their development is still hindered by the lack of cheap and bright single photon sources (SPSs) operating at room temperature (RT). In this paper, we show the occurrence of photon antibunching at RT from single colloidal CdSe/ZnS nanocrystals (NCs) inserted in a vertical microcavity. Moreover, by using high-resolution lithographic techniques, we conceived a general route for positioning single colloidal quantum dots in the microcavity. The findings and the technique presented here can be considered a first step towards the development of SPS devices operating at RT.

[4] Author to whom any correspondence should be addressed.

Contents

1. Introduction

The theorization of quantum cryptography and quantum key distribution as effective routes for the transmission of highly sensitive data fostered the development of communication systems based on the generation, manipulation and detection of single photons transporting binary-coded information. Among the proposed sources of single photons [1]–[3], major efforts have been made towards epitaxially grown quantum dots (QDs) [4, 5], although the maximum operating temperature of epitaxial QD-based single photon sources (SPSs) is still far from room temperature (RT) conditions [6]. Among the possible alternatives to epitaxial QDs, molecular dyes [7]–[9], defects in solids [10]–[12] and colloidal NCs [13]–[17] are considered good candidates for development of SPS operating at RT. In particular, wet chemistry-based colloidal NCs represent the most promising materials, due to several appealing characteristics, such as low fabrication costs, high versatility in the chemical synthesis, broad tunable emission range (from visible to infrared) [18] and high quantum efficiency at RT (up to 98%) [19]. Most importantly, these nanomaterials have a high Auger recombination rate [16], and consequently a low probability for multiphoton emission, the latter being an essential requirement in SPS devices. Nevertheless, peculiar features of colloidal NCs, such as blinking, low collimated emission, nonpolarized emission and long luminescence lifetimes [20, 21], still prevent their application to single-photon emitting devices, although several strategies are being investigated to overcome this limitation by controlling the nanocrystal (NC) emission at the single molecule level [14], [22]–[24]. In particular, the insertion of the emitters in quantum-confined optical resonators [25, 26] seems to be the most effective way to engineer their radiative decay and to control the radiative pattern (thus enabling an efficient coupling into fibers). Moreover, the peculiar unpolarized emission of spherical NCs [27, 28] allows for their efficient coupling to the cavity modes, regardless of the polarization of the latter [29], once they are inserted in the resonator. For this purpose, the difficulty to position them precisely in a cavity is still a challenge to overcome.

Here, we show the effectiveness of a general way for the fabrication of SPSs operating at RT. By means of high-resolution lithographic techniques, we were able to isolate single NCs in a planar microcavity. Spectroscopic characterization points out the typical antibunching behavior and shortening of the spontaneous emission lifetime, demonstrating the success of the employed method.

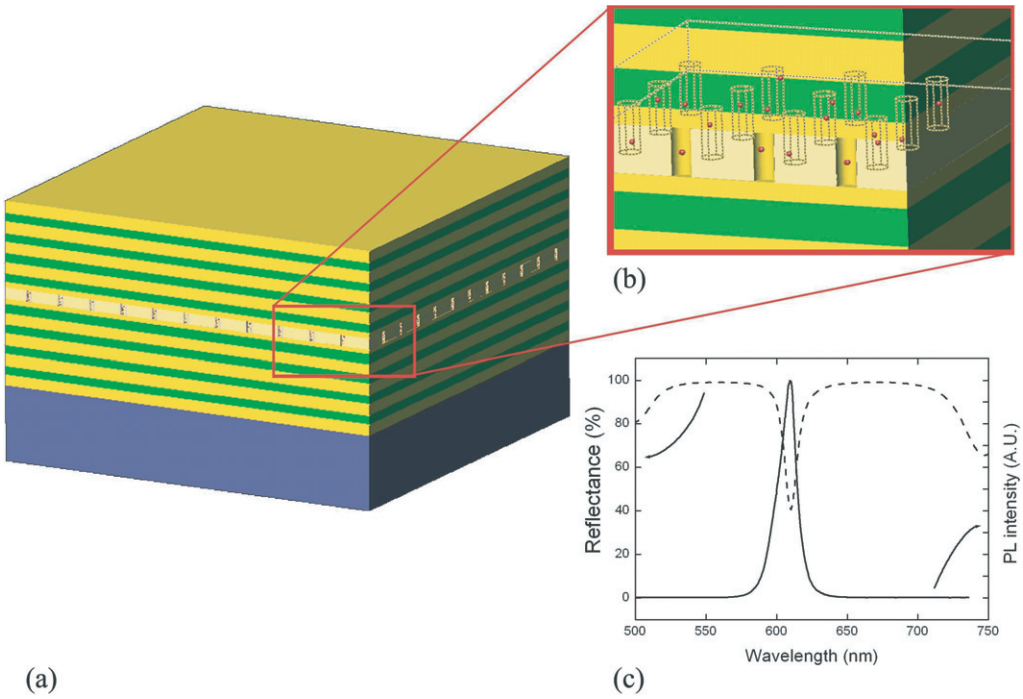

Figure 1. (a, b) 3D sketches of the whole structure and of the cavity region, respectively. (c) Reflectance spectrum (dashed line) measured from the top of the device, as compared with the PL of a NC ensemble (solid line) collected from a 500 nm-wide pillar.

2. Materials and methods

Colloidal semiconductor CdSe/ZnS NCs emitting at 610 nm (diameter ∼5.2 nm) were purchased from Evident Technology in toluene solution, while the electronic resist hydrogen silsesquioxane (HSQ) was purchased from Dow Corning Company. The NCs were previously precipitated and re-diluted in methylisobutylketone (MIBK) solvent before dispersion in the electronic resist. A molar concentration of $C_{NC} \sim 10^{-7}$ mol l^{-1} in the resist solution was used in order to obtain a low surface density of the emitters after spin coating.

2.1. Processing method

The design of the distributed Bragg reflectors (DBRs) and of the microcavity was performed through simulations based on the transfer matrix method. Finite-difference time-domain (FDTD) calculations also confirmed the spatial distribution of the resonant mode in the cavity.

A DBR consisting of four alternating quarter-wavelength thick layers of SiO_2/TiO_2 and an additional SiO_2 spacing layer (62 nm thick) were preliminarily grown on a silicon substrate by electron-beam evaporation. A low concentration (10^{-7} mol l^{-1}) of NCs was dispersed in a high-resolution electron-beam resist (HSQ) [30]. A 90 nm thick layer of the blend was spin-coated on the dielectric structure and subsequently exposed to the electron beam. Arrays of active pillars (see sketches of figures 1(a) and (b)) were defined using a RAITH 150 e-beam lithography (EBL) system operating at 20 kV. In order to reduce both the feature sizes and the exposure time, the EBL system was used in single-point exposure. In this way, by tuning the exposure

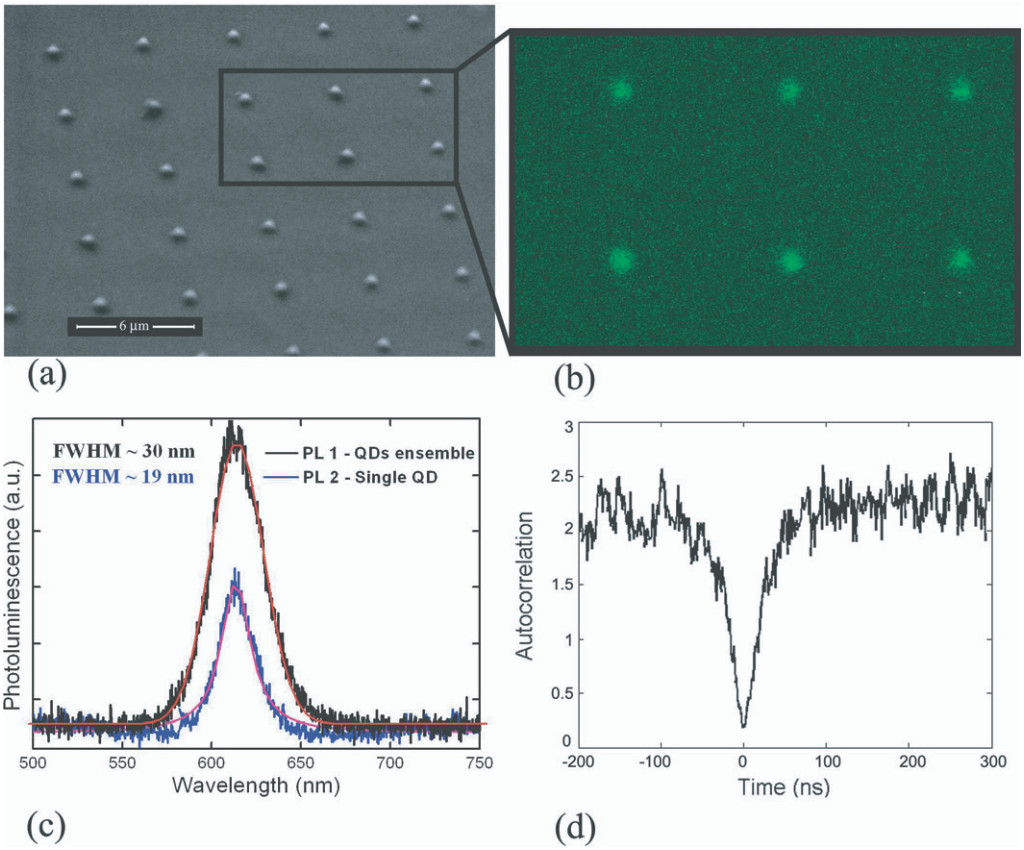

Figure 2. (a) SEM image of the fabricated pattern (details of the region containing pillars with a diameter of 500 nm). (b) PL map collected from the same region. (c) PL spectra showing the different line-shape depending on the different dimensions of the pillars (black line collected from a 500 nm-wide pillar and blue line collected from a 90 nm-wide pillar). (d) Auto-correlation trace of the PL arising from a 90 nm-wide pillar (normalized with background correction), showing an antibunching behavior.

dose, high-quality arrays of pillars with diameters ranging from 30 nm up to 500 nm (figure 2(a)) and a period of 6 μm were realized. As previously reported [31], ensembles of NCs embedded in electronic resists can be easily patterned by means of traditional lithographic processes, since the presence of semiconductor clusters in the matrix does not significantly affect the sensitivity of the polymeric host and, at the same time, the emission characteristics of the NCs are not modified by the interaction with the electron beam. Subsequently, the array of localized single quantum emitters was clad by a second DBR consisting of four alternating quarter-wavelength thick layers of TiO_2/SiO_2. The complete planar microcavity is sketched in figure 1(a) (the detail of the cavity region is shown in figure 1(b)). To guarantee a preferential field penetration along the vertical direction into the DBR layers, a flattening layer of pure HSQ was spin-coated on the active region before the deposition of the top mirror [32]. Moreover, the central region was completed by two SiO_2 spacing layers, below and above the flattened pillars, in order to locate the emitters close to the antinodal position of a $\lambda/2$ cavity.

2.2. Spectroscopic characterization

The overall reflectivity of the grown planar microcavity was measured using a Varian Cary 5000 Spectrophotometer.

Micro-photoluminescence and imaging measurements were performed on the grown sample with an Olympus Fluoview-1000 confocal microscope coupled to a nitrogen-cooled Si-CCD through a 33 cm long monochromator. The sample was excited in CW by means of a laser diode emitting at 405 nm. Highly spatially resolved measurements (spatial resolution up to 200 nm) allowed the emission spectrum from the nanometer-sized pillars to be collected, with an integration time of 20 s.

To investigate in detail single photon emission, we used a confocal microscope coupled to a standard high sensitivity Hanbury-Brown and Twiss set-up. It is based on two avalanche photodiodes (Perkin Elmer SPCM AQR 13) with a time resolution of 300 ps. The electrical pulses from the photodiodes are sent to a data acquisition card (TimeHarp 200) for time-resolved analysis.

This card records the stop events during 4.7 μs after a start pulse with a time resolution of 1.1 ns. To investigate negative correlation times, a constant delay ($\sim$200 ns) was introduced in the stop channel. The recorded data enable the acquisition of the histogram of the delays between photons. In this case, the excitation light came from a pulsed laser diode (LDH-P-C, Picoquant, pulses duration in the picosecond range, wavelength 404 nm and repetition rate ranging between 2.5 and 40 MHz), whose beam was focused on the sample by the high numerical aperture objective (NA $=$ 0.95) of the microscope.

One of the aims of the present work was to assess the possible effect of the microcavity on the PL lifetime of the NCs. Therefore, all the measurements were performed before and after the growth of the upper DBR, by keeping the sample at RT.

3. Results and discussion

Figure 1(c) shows the overlap of the reflectivity and the PL spectra, as collected from the top of the device at RT. The microcavity was designed to resonate at a wavelength of 610 nm, as confirmed by the cavity dip in the measured reflectance spectrum (dashed line). The PL spectrum (solid line) was collected from a 500 nm-wide pillar embedding an ensemble of CdSe/ZnS QDs. The cavity modulation effect on the spontaneous emission is demonstrated by the narrowing of the PL line width down to 14.6 nm. The slight broadening of the PL line-shape, as compared with the dip measured in the reflectance spectrum, could be attributed both to the increased optical losses in the cavity due to the absorption and/or scattering of the nanoclusters and to the different numerical aperture of the spectroscopic systems employed. The observed small spectral shifts of the resonant emission have been attributed to local variations of the spin-coated layer that determines the cavity thickness and therefore its resonant wavelength.

The morphological and optical analysis of the structure without the top DBR is reported in figure 2. The scanning electron microscope (SEM) image in figure 2(a) is an example of the fabricated array of pillars (the region containing the largest pillars with a diameter of 500 nm is reported). In figure 2(b), the fluorescence map of the same region shows photoluminescence (PL) only from the areas corresponding to the pillar sites, thus confirming the effectiveness of the localization process of the NCs on the DBR. Interestingly, the PL line-shape changes depending on the different dimensions of the pillars. Structures having a

diameter above 100 nm showed a Gaussian profile, typical of an ensemble of NCs, with a full-width at half-maximum (FWHM) of about 30 nm (figure 2(c), black line). In contrast, narrower emission (FWHM ∼19 nm) was collected from the smallest ones (figure 2(c), blue line). Moreover, it assumed a Lorentzian profile [33][5] and presented the typical intermittent emission [20] (not shown here), indicating that the PL arises from single NCs. By analyzing the auto-correlation function of the emitted signal from single NCs (figure 2(d)), we found a photon antibunching behavior [23] of the luminescence, a clear fingerprint of the single photon nature of the studied NCs. The lifetime obtained from the analysis of the coincidence counts is about 23 ns, comparable with typical radiative time constants of colloidal CdSe/ZnS NCs [16]. This suggests that embedding the NCs in HSQ does not generate extra nonradiative recombination channels due to the modification of the NC surface.

Figure 3 reports the optical characterization of single NCs in a microcavity, after deposition of the top mirror. Figure 3(a) shows a representative PL spectrum of a single NC recorded from a 90 nm-wide pillar. Its line width is further reduced down to 12.3 nm with respect to the luminescence of an ensemble of NCs in the cavity (14.6 nm), since the presence of a single semiconductor emitter in the pillar causes lower absorption and scattering losses. The evidence for single photon generation is given, also in this case, by measurement of the autocorrelation function of the emitted light, which reveals an antibunching behavior at zero delay (see figure 3(b)).

The area of the peak at zero delay is equal to 0.27. After subtracting the signal corresponding to the background, this area is even lower with a value of 0.21. The normalized area of the peaks at nonzero delays goes up to 1.35, reflecting an additional bunching of the fluorescence due to the emission intermittency. Despite the fact that the measurements were performed at low excitation density (pulses are collimated at the diffraction limit with an energy of the order of tens of fJ with a repetition rate of 10 MHz) the peak at zero delay presents a nonzero signal, probably due to unavoidable residual laser light scattered by the top mirror.

Using the histogram of the coincidence counts, we deduced the lifetime of the excited state [16]. The exponential fit of the experimental data collected from several NCs gives an average radiative lifetime of $\tau_{cav} \sim 9.1$ ns. In figure 3(c), a representative PL decay curve, black squares, in comparison with that of single NCs surrounded by HSQ (black disks), not inserted in the microcavity (without top mirror, average lifetime $\tau_{fs} \sim 23$ ns), is reported. Since the single NCs examined were embedded in the same material, we can exclude the possibility that the shortening of the lifetime is related to additional nonradiative relaxation mechanisms introduced by depositing the top mirror. On the contrary, as the NCs have a quantum efficiency close to 1 [19], the ratio $\tau_{fs}/\tau_{cav} \cong 2.4$ can be considered as modification of the radiative lifetime due to the wavelength-sized cavity. The redistribution of the optical mode density due to the light quantum-confinement in the cavity, indeed alters the radiation properties of an electric dipole, thus increasing or decreasing its spontaneous emission rate depending on the orientation of the dipole and whether its oscillation frequency is resonant with the cavity or not [34]. Theoretically, it has been calculated that the enhancement of the radiative decay rate for an emitter behaving as a linear dipole in an ideal $\lambda/2$ cavity with 100% reflecting mirrors ranges between 1.5 (dipole perpendicular to longitudinal axis of the cavity) and 3 (dipole parallel to the longitudinal axis) [34, 35]. Taking into account the 2D

[5] The relatively high FWHM of the PL signal (about 19 nm) is due to the combination between the well-known spectral diffusion process and the high integration time (20 s) needed for RT measurements (as reported, for example, in [33].

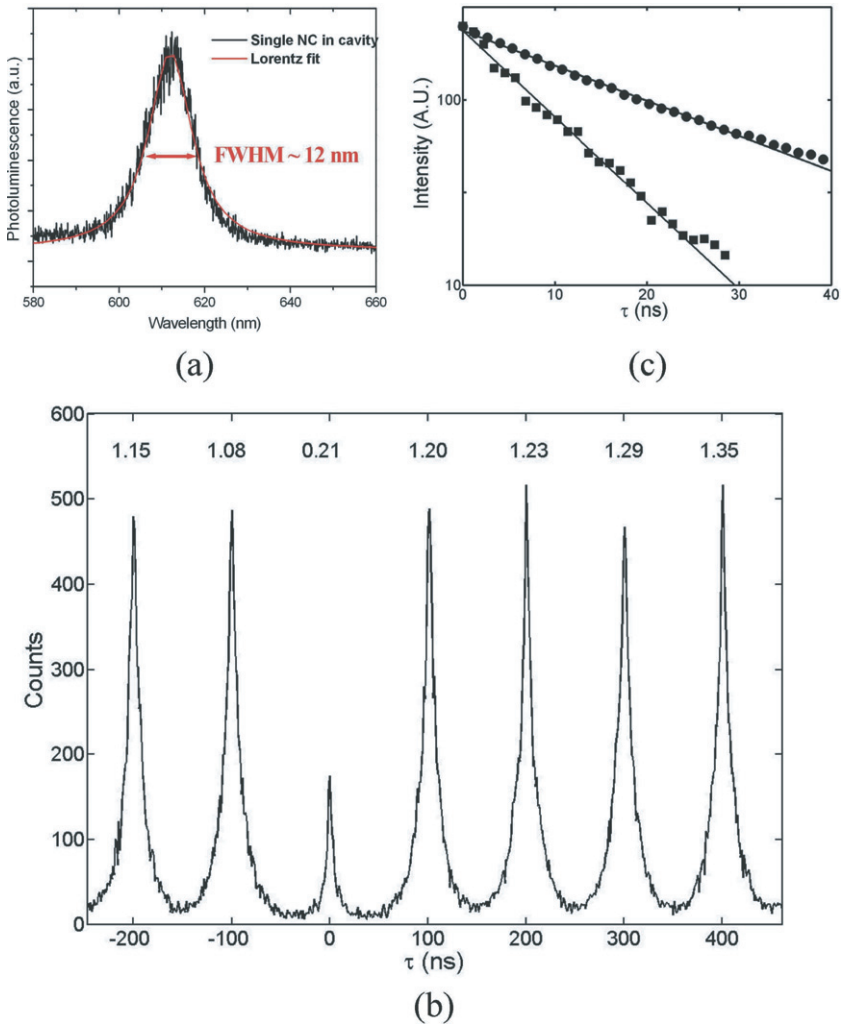

Figure 3. (a) RT PL of a 90 nm-wide pillar. (b) Histogram of coincidence counts of a single QD fluorescence. Above each peak, the area normalized to Poissonian photon statistics, with background correction, is given. (c) PL decay corresponding to the peak at 100 ns delay plotted in (b) (squares) and to an ensemble of NCs surrounded by HSQ not inserted in a cavity (circles).

degenerate structure of the NC emitting dipole, the expected enhancement ranges between 2.25 and 3, and is in very good agreement with respect to our experimental findings.

The unprecedented antibunching behavior observed from colloidal NCs embedded in a planar microcavity, together with an efficient tailoring of the recombination decay rate at RT, confirms the suitability of this approach for the fabrication of SPSs based on colloidal NCs, thus overcoming the limitation in the operating temperature shown by epitaxial QD sources. This approach applied to recently proposed architectures for colloidal NCs-based organic light emitting diodes [36] would open the way to both the realization of electrically injected NC-based SPSs and a 3D quantization of the optical modes, by embedding the NC in high index nanopillars, a simpler technological alternative to micropost devices [37] obtained by deep-etching techniques.

4. Conclusions

In summary, we investigated the possibility of obtaining SPSs through the insertion and localization of single colloidal NCs in a vertical microcavity, by high-resolution lithographic techniques. By means of confocal optical spectroscopy, we demonstrated the effectiveness of the approach employed, and reported the first single photon emission from an individual colloidal NC inserted in a microcavity, at RT. Moreover, the lifetime measurement of single NCs shows an enhancement in their radiative rate when introduced into the cavity. These findings open the way for the exploitation of colloidal NCs as real SPSs operating at RT.

By engineering the insertion of single NCs in a cavity, remarkably higher control over their emission properties, such as the lifetime decay and the radiative pattern, can be achieved. This should lead, for instance, to a faster frequency modulation of the single-photon emission and to a more efficient coupling into fiber networks [34] or into low numerical aperture collection systems, and will be subject of future work.

Acknowledgment

We gratefully thank Gianmichele Epifani, Gianvito De Iaco and Angelo Melcarne for their expert technical help.

References

[1] Kurtsiefer C, Mayer S, Zarda P and Weinfurter H 2000 *Phys. Rev. Lett.* **85** 290
[2] Brunel C, Lounis B, Tamarat P and Orrit M 1999 *Phys. Rev. Lett.* **83** 2722
[3] Hennrich M, Legero T, Kuhn A and Rempe G 2004 *New J. Phys.* **6** 86
[4] Pelton M, Santori C, Vucković J, Zhang B, Solomon G S, Plant J and Yamamoto Y 2002 *Phys. Rev. Lett.* **89** 233602
[5] Hennessy K, Badolato A, Winger M, Gerace D, Atatüre M, Gulde S, Fält S, Hu E L and Imamoğlu A 2007 *Nature* **445** 896
[6] Kako S, Santori C, Hoshino K, Götzinger S, Yamamoto Y and Arakawa Y 2006 *Nat. Mater.* **5** 887
[7] Moerner W E 2004 *New J. Phys.* **6** 88
[8] Lukishova S G, Schmid A W, Knox R, Freivald P, Bissell L J, Boyd R W, Stroudud C R and Marshall K L 2007 *J. Mod. Opt.* **54** 417
[9] Lukishova S G, Knox R P, Freivald P, McNamara A, Boyd R W, Stroud C R, Schmid A W and Marshall K L 2006 *Mol. Cryst. Liq. Cryst.* **454** 1
[10] Wu E, Jacques V, Treussart F, Zeng H, Grangier P and Roch J F 2006 *J. Lumin.* **119** 19
[11] Gaebel T, Popa I, Gruber A, Domhan M, Jelezko F and Wrachtrup J 2004 *New J. Phys.* **6** 98
[12] Wu E, Rabeau J R, Roger G, Treussart F, Zeng H, Grangier P, Prawer S and Roch J-F 2007 *New J. Phys.* **9** 434
[13] Lounis B, Bechtel H A, Gerion D, Alivisatos P and Moerner W E 2000 *Chem. Phys. Lett.* **329** 399
[14] Messin G, Hermier J P, Giacobino E, Desbiolles P and Dahan M 2001 *Opt. Lett.* **26** 1891
[15] Brokmann X, Giacobino E, Dahan M and Hermier J P 2004 *Appl. Phys. Lett.* **85** 712
[16] Brokmann X, Messin G, Desbiolles P, Giacobino E, Dahan M and Hermier J P 2004 *New J. Phys.* **6** 99
[17] Martiradonna L, Carbone L, Tandaechanurat A, Kitamura M, Iwamoto S, Manna L, De Vittorio M, Cingolani R and Arakawa Y 2008 *Nano Lett.* **8** 260
[18] Murray C B, Norris D J and Bawendi M G 1993 *J. Am. Chem. Soc.* **115** 8706
[19] Brokmann X, Coolen L, Dahan M and Hermier J P 2004 *Phys. Rev. Lett.* **93** 107403
[20] Neuhauser R G, Shimizu K T, Woo W K, Empedocles S A and Bawendi M G 2000 *Phys. Rev. Lett.* **85** 3301

[21] Schlegel G, Bohnenberger J, Potapova I and Mews A 2002 *Phys. Rev. Lett.* **88** 137401
[22] Hohng S and Ha T 2004 *J. Am. Chem. Soc.* **126** 1324
[23] Brokmann X, Coolen L, Hermier J P and Dahan M 2005 *Chem. Phys.* **318** 91
[24] Pompa P P, Martiradonna L, Della Torre A, Della Sala F, Manna L, De Vittorio M, Calabi F, Cingolani R and Rinaldi R 2006 *Nat. Nanotechnol.* **1** 126
[25] Purcell E M 1946 *Phys. Rev.* **69** 681
[26] Artemyev M V, Woggon U, Wannemacher R, Jaschinski H and Langbein W 2001 *Nano Lett.* **1** 309
[27] Califano M, Franceschetti A and Zungr A 2007 *Phys. Rev.* B **75** 115401
[28] Crooker S A, Barrik T, Hollingsworth J A and Klimov V I 2003 *Appl. Phys. Lett.* **82** 2793
[29] Silva A G *et al* 2008 *Opt. Express* **16** 19201
[30] Namatsu H, Yamaguchi H, Nagase T, Yamazaki M and Kurihara K 1998 *Microelectron. Eng.* **41** 331
[31] Martiradonna L, Stomeo T, De Giorgi M, Cingolani R and De Vittorio M 2006 *Microelectron. Eng.* **83** 1478
[32] Plakhotnik T 2005 *Opt. Express* **13** 3049
[33] Empedocles S A *et al* 1999 *Adv. Mater.* **11** 1243
[34] Yokoyama H 1992 *Science* **256** 5053
[35] Bjork G 1994 *IEEE J. Quantum Electron.* **30** 2314
[36] Li Y Q, Rizzo A, Cingolani R and Gigli G 2006 *Adv. Mater.* **18** 2545
[37] Kahl M *et al* 2007 *Nano Lett.* **7** 2897